Low Temperature Physics/Fizika Nizkikh Temperatur, 2019, v. 45, No. 6, pp. 701–709

New possible route of HC_3N formation in Titan's atmosphere

J. Mouzay, C. Assadourian, N. Piétri, T. Chiavassa, and I. Couturier-Tamburelli

Aix-Marseille Université, CNRS, PIIM, UMR 7345, Marseille 13397, France
E-mail: isabelle.couturier@univ-amu.fr

Received January 31, 2019, published online April 26, 2019

The structures of the C_2N_2/C_2H_2 complex in solid argon matrices have been investigated using FTIR spectroscopy and *ab initio* calculations, at the aug-cc-pVTZ level of theory. Predicted frequency shifts for the linear structure, characterized by a strong hydrogen bond between the nitrogen of C_2N_2 and the acetylenic proton were found in good agreement with the ones from the experiment. The photodissociation of C_2N_2–C_2H_2 complex trapped in argon matrix at 10 K has been performed at 120 nm. The FTIR measurement and *ab initio* calculations pointed to the formation of HC_3N, HCN and probably HC_2NC and HNC as final reactional products. This mechanism route is potentially important for chemical models of the Titan's atmosphere.

Keywords: argon matrices, Titan's atmosphere, FTIR spectroscopy.

Introduction

Titan, the largest moon of Saturn, is the only satellite in the solar system to have a dense atmosphere. Unlike Earth, Titan's atmosphere is oxygen-deficient, but predominantly composed of nitrogen and a few percent of methane [1]. In Titan's upper atmosphere, N_2 and CH_4 are photodissociated by different sources of radiations as solar wind particles and ultraviolet radiations, leading to the formation of nitriles and hydrocarbons [2]. Among the detected molecules, cyanogen (C_2N_2) and acetylene (C_2H_2) are present in a large proportion [3] and can lead to the formation of complex molecules by molecular growth (under photochemical radiation) [3c,4]. In particular, both molecules are the small precursors to synthesize unsaturated linear molecules like cyanopolyynes ($HC_{2n+1}N$) whose first members like HC_3N and HC_5N are detected in Titan's atmosphere [4a,3b,c]. The formation of cyanopolyynes in space most probably involves the collisions of neutral radicals $CN^{\bullet}$ with polyacetylenic hydrocarbons ($HC_{2n}H$) or more generally, of $^{\bullet}C_{2n+1}N$ radicals with $HC_{2n}H$ molecules [5]. This was demonstrated by Balucani *et al.* [6] in a crossed molecular beam experiment, which consisted in the cyanoacetylene production from acetylene and ground state cyano radicals $CN^{\bullet}$ coming from HCN or C_2N_2 as illustrated in various models [7]. Numerous experiments [8,9] on the photolysis of C_2H_2 performed at various photolysis wavelengths (193.3 nm [6–10]; 184.9 nm [11]; 147 nm [12]; 123.6 nm [13] and 121.6 nm [14]) are reported in the literature. According to the photolysis wavelengths used, these studies show that the major primary photochemical process is different. Lauter *et al.* [14] have proved that the dissociation dynamics of acetylene after photoexcitation at the Lyman-α wavelength (121.6 nm) induces the formation of $H^{\bullet}$ atoms along with $^{\bullet}C_2H$ radicals as the main photochemical process.

The cyanogen molecule has also been extensively studied experimentally [15–20] and became a model for photochemical studies as a source of $^{\bullet}CN$ radicals.

Numerous studies on the photochemical synthesis used IR spectrometry as a detection method of molecules trapped in cryogenic rare gas matrix. This latter offers a convenient laboratory environment for spectroscopic studies on isolated intermolecular complexes. Recent studies demonstrated that the cryogenic co-deposition of HC_5N/HC_2H [21], HC_3N/HC_4H [22], C_4N_2/HC_2H [23], HC_3N/HC_2H [23], or HC_2H/HCN [24] induces the formation of the well-defined complexes. The combination of experimental and theoretical informations showed that the hydrogen-bond system involving C–H···π interaction plays a significant role in determining the shape or the conformation of molecules in the matrix. There are two approaches of complex; (i) linear complex showing the interaction between the nitrogen atom of X–CN and one hydrogen atom of $HC_{2n}H$ moiety and (ii) *P*-complex formed by the π-electron of X–CN and the π-electron of acetylenic molecules. Considering the major photodissociation processes of the two molecules involved in the complex, previous studies [5] showed that these kinds

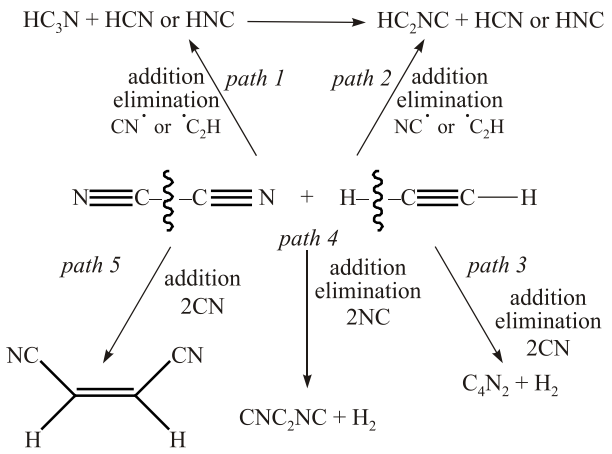

Scheme 1. Proposed mechanism reaction of C_2H_2/C_2N_2 complex under photolysis performed at $\lambda > 120$ nm.

of molecular complexes could be considered as the pre-reactive states which can lead to routes to the more long-chained molecules synthesis.

In this paper we first report the characterization of pre-reactive states between C_2H_2 and C_2N_2 using computational method. Secondly, we describe the photochemistry of C_2H_2:C_2N_2 complex which can induce the formation of different products by addition ($C_4H_2N_2$, path 5) or addition/elimination (HC_3N; HC_2NC; HCN, C_4N_2, path 1 to 4) processes presented in Scheme 1. The goal is to confirm the mechanism route leading to the formation of HC_3N as illustrated by the chemical models of Titan's atmosphere [7].

2. Experiment

Pure acetylene was supplied by Air Liquid (purity 99.6%) and was used without further purification. Pure cyanogen was prepared in a flask containing AgCN (20 g, 15 mmol) that was adapted to a U-tube equipped with stopcocks in a vacuum line (10^{-2} mbar). The U-tube was immersed in a liquid nitrogen bath and the flask was heated with a Bunsen burner for around 2 min to form, via the cyanogen radical, the cyanogen molecule NCCN which was trapped in the U-tube. The stopcocks of the U-tube were then closed and the cyanogen was obtained.

Matrix isolation experiments. The apparatus and experimental techniques used to obtain argon matrices have been described previously [25]. Gas mixtures were prepared using standard manometric techniques. The C_2H_2/Ar and C_2N_2/Ar mixtures are prepared in a 0.5/500 and 1/500 ratio, and the C_2H_2/C_2N_2/Ar mixture is prepared in a 2/1/500 ratio. The gas mixture is sprayed onto a gold-coated copper plate cooled down to 20 K with the help of a cold head cryostat (CTI, model 21) with a high vacuum chamber (ca 10^{-7} mbar). A Fourier transform infrared spectrometer (Nicolet series II Magna system 750) was used to record the reflexion-absorption spectra of samples at 10 K in the 4000–650 cm^{-1} range. Each spectrum has a spectral resolution of 0.125 cm^{-1}.

Irradiation techniques. All cryogenic samples were irradiated using a microwave discharge H_2 lamp (Opthos Instruments), which simulated the interstellar radiation field and was adapted directly onto the sample chamber. The spectral flux of the lamp (operated with a steady flow of hydrogen, at 0.9 mbar) was confined in the range 3–10 eV, being dominated by two bands centred on 120 and 160 nm, approximately $(4.79\pm1.37)\cdot10^{13}$ photons·cm^{-2}·s^{-1} [26]. The flux of the lamp was transmitted through an MgF_2 window ($\lambda > 120$ nm).

Details of calculations. Quantum chemical calculations were carried out with Gaussian 09 [27]. The equilibrium structure of C_2H_2, C_2N_2 and their complexes as well as the corresponding harmonic frequencies of molecular vibrations (as given by analytical second derivatives of the total energy, with respect to nuclear positions) were predicted using the density functional theory (DFT) [28] with the B3LYP hybrid exchange correlation functional [29], the correlation-consistent polarized valence triple-ξ basis set augmented by *s*, *p*, *d*, and *f* functions (aug-cc-pVTZ) [30], and standard convergence criteria.

3. Results and discussion

Figure 1 shows the spectra recorded at 10 K after an annealing to 30 K for C_2H_2 (Fig. 1(a)), C_2H_2/C_2N_2/Ar (Fig. 1(b)) and C_2N_2/Ar (Fig. 1(c)) in three spectral regions. In these spectra, each vibrational mode exhibits multiple absorption lines due to different matrix sites and polymeric compounds.

3.1. C_2N_2 *and* C_2H_2 *isolated in argon matrix*

Acetylene is a linear molecule with three strong absorption bands in its infrared spectrum observed in Ar matrix at 3302.8, 3289.1 and 736.9 cm^{-1}. The two first correspond to a Fermi-resonance involving the $\nu_2 + \nu_4 + \nu_5$ and the ν_3 vibrations (Fig. 1(a)). The last one observed at 736.9 cm^{-1} is assigned to the ν_5 mode of acetylene (Fig. 1(a)) [31].

Numerous works on the IR absorption spectrum of gaseous [32] and solid [33] cyanogen C_2N_2 have already been published. The Raman spectrum of liquid cyanogen has also been measured [34]. This compound is likewise a linear centrosymmetric molecule ($D\infty h$ point group) with seven normal modes of vibration. Among these modes, only the CN antisymmetric fundamental stretching (ν'_3) (Fig. 1(c)) is infrared active and could be present between 4000–400 cm^{-1}. In our experimental conditions (Fig. 1(c)), four bands are observed at 2153.9, 2657.2, 2559.6 and 742.1 cm^{-1}. The first one corresponds to the CN antisymmetric stretching mode (ν'_3). The three others correspond respectively to combination modes involving the $\nu'_3 + \nu'_4$, $\nu'_1 + \nu'_5$ and $\nu'_4 + \nu'_5$ vibrational absorptions.

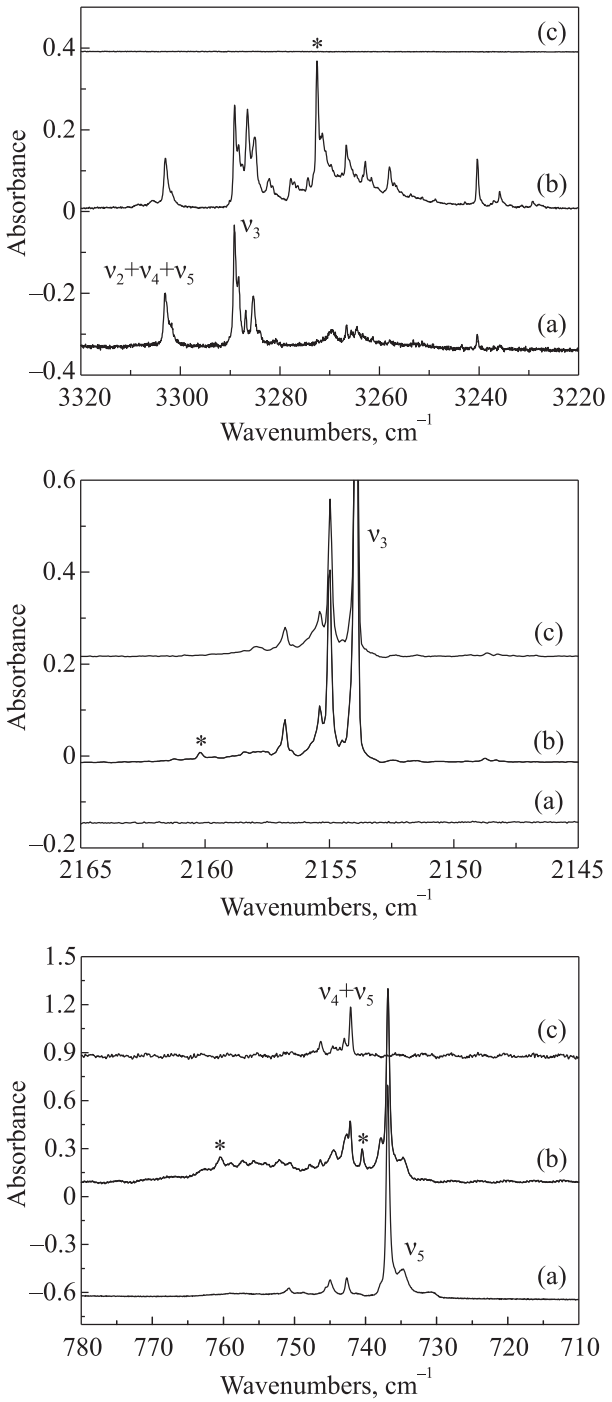

Fig. 1. FTIR spectra at T = 10 K after 30 K annealing of C_2H_2/Ar in a 0.5/500 ratio (a), C_2N_2/C_2H_2/Ar in a 2/1/500 ratio T = 10 K (b), C_2N_2/Ar in a 1/500 ratio T = 10 K (c). The most intense bands of the molecular complexes are noted with an asterisk. In these spectra, each vibrational mode exhibits multiple absorption lines due to different matrix sites and polymeric compounds.

3.2. C_2N_2/C_2H_2 *codeposition in argon matrix*

Figure 1(b) gives an overview of the spectrum in the 3320–3220, 2170–2160 and 780–715 cm^{-1} areas obtained when the cyanogen and C_2H_2 are codeposited in argon matrix. The spectrum shows the absorption bands of monomers and homopolymers attributed by comparison of this spectrum with those of the monomers obtained at 10 K (Fig. 1(a) and 1(c)), but also other new absorption bands noted by an asterisk in Fig. 1(b). According to previous studies, we can expect the formation of a complex between C_2N_2 and C_2H_2. Annealing of the matrix to 30 K induces an increase in the intensity of these bands and a decrease of those assigned to the isolated molecules. When the temperature increases, the trapping sites are reorganized, promoting the formation of the complex. It is well known that the complexation between two molecules induces the formation of new bands which are shifted compared to those of the monomers. To identify the geometry of the complex formed, we have to calculate these shifts for all the fundamental modes by comparison of the new bands with those of the monomers ($\Delta\nu$ ($\nu_{monomer}-\nu_{complex}$)). Among these bands, one is observed in the CN stretching range of C_2N_2 at 2160.2 cm^{-1} (Fig. 1(b)) shifted to higher frequency by 6.3 cm^{-1} with respect to the ν_3' of C_2N_2. Two other bands are observed at 2345 cm^{-1} and 860.1 cm^{-1}. These bands are observed respectively in the ν_1' and ν_2' mode range of C_2N_2. For these modes, it is difficult to determine the frequency shifts induced by the complexation because the absorption bands of monomers are not IR active.

Likewise, in the acetylenic CH bond stretching range, we observe one new band at 3272.5 cm^{-1} shifted to lower frequencies by –16.6 cm^{-1} compared to the 3289.1 cm^{-1} mode of C_2H_2 monomer. On the other hand, in the 710–780 cm^{-1} range (Fig. 1(c)), we observe two absorption bands at 759.8 cm^{-1} and 740 cm^{-1}. These bands growing in the $\nu_4' + \nu_5'$ mode range of C_2N_2 and the ν_5 mode area of C_2H_2, we have to compare their shifts with these two vibrational modes. So, the band observed at 759.8 cm^{-1} is shifted to higher frequency by 22.9 cm^{-1} with respect to the ν_5 mode of C_2H_2 and 17.7 cm^{-1} if we consider the $\nu_4' + \nu_5'$ mode of C_2N_2. On the other hand, the band observed at 740 cm^{-1} is either shifted to higher frequency by 3.1 cm^{-1} compared to the ν_5 mode of C_2H_2 or to lower frequency by –2.1 cm^{-1} compared to the $\nu_4' + \nu_5'$ mode of C_2N_2.

3.3. Theoretical study

Our experimental results indicate the formation of a complex between C_2N_2 and C_2H_2. To establish the molecular structure, theoretical calculations have been performed with Gaussian 09 at the B3LYP level with aug-cc-pVTZ basis sets. Several arrangements are possible in the complex subunits. If we consider the Mulliken's charges (Scheme 2), one hydrogen atom of acetylene is expected to be involved in an H-bond interaction with C_2N_2 by the nitrogen atom (linear structure). We also investigated a parallel complex structure by analogy with the complex formed between C_2H_2 and C_4N_2 [23] or C_3O_2 [35] and previous studies developed in our laboratory [36].

From these initial configurations, calculations yield to two local minima. The optimized structures are shown in

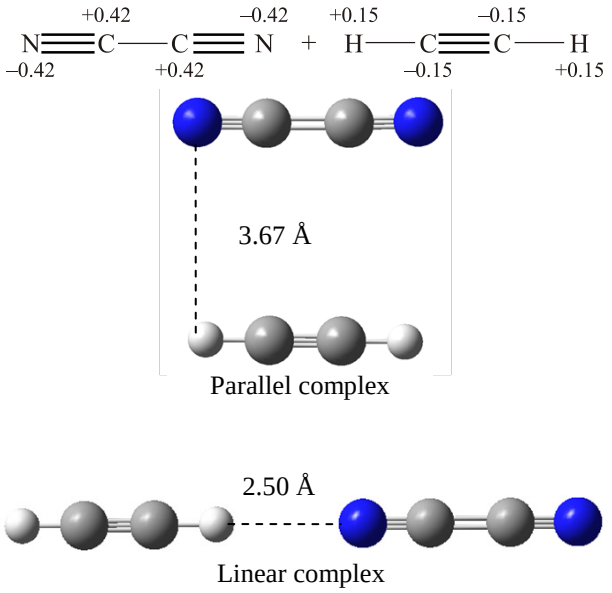

Scheme 2. Mulliken's charges of acetylene and cyanogen and structure of optimized complexes.

Scheme 2. The first minimum corresponding to the linear shape exhibits a hydrogen bond between C_2H_2 and C_2N_2 moieties which is estimated to 2.50 Å in aug-cc-pVTZ, by calculation. For the C_2N_2 and C_2H_2 subunit in comparison to the monomers, we observe, respectively, a slight shortening of the CN bond (r = 0.001 Å) and a lengthening of C–H bond (0.002 Å). The second minimum corresponds to the parallel structure. In this complex, the acetylene and the cyanogen axes are parallel; the two acetylenic hydrogens are adjacent to the nitrogen of the cyanogen (3.67 Å). The geometrical parameters are similar to those of the monomer. The linear complex is predicted to be most stable with respect to the monomers (5.2 kJ·mol^{-1}), but the energy 2.07 kJ·mol^{-1} regarding to the parallel complex is not significant at this level of theory into clearly determining the structure present in argon matrix. It is therefore appropriate to compare the experimental frequency shifts induced by the complexation with those calculated (Table 1).

The theoretical calculations provide valuable information's on the stability and the spectroscopic features of the complexes. The complexation effects can be observed on the geometry of the partner molecules and on the corresponding bond stretching vibrational frequencies (Table 1). The geometric parameters being slightly modified by the complexation, we observe minor and similar shifts for the C_2N_2 subunit in the P- or L-complex. For example the C_2N_2 ν'_3 mode is predicted to be shifted by +3.9 cm^{-1} and +1.4 cm^{-1} for the L- and P-complexes respectively and the experimental one has been found to be +6.3 cm^{-1}. The comparison between experimental and calculated shifts on C_2N_2 does not allow the identification of the form present in argon matrixes (Table 1).

On the other hand the C_2N_2/C_2H_2 interaction induces an important calculated frequency shift of the ν_5 deformation mode of C_2H_2 towards higher frequencies (+35 cm^{-1}) in the L-complex while the P-complex indicates a shift towards higher frequencies of only around 4 cm^{-1} (+4.9 or 4.3 cm^{-1}). The shift calculated for the L-complex is in better agreement with the experimental one +22.9 cm^{-1} showing as well as the band observed at 759.8 cm^{-1} is a response of the ν_5 mode of C_2H_2. The L-complex is indeed characterized by a large shift for the 3289.1 cm^{-1} mode of C_2H_2. This mode is moved to lower frequency by –13.6 cm^{-1}, with respect to the monomer while it is slightly shifted –3.8 cm^{-1} in the P-complex. The experimental shift being –16.6 cm^{-1}, we can say that the calculated frequency shifts for the L-complex are in good agreement with this result. So, we can conclude that this L-complex is present in argon matrix.

As discussed in the Sec. 3.2, the band observed at 740 cm^{-1} can be attributed to the C_2H_2 complexed ν_5 mode or at the combination $\nu'_4 + \nu'_5$ mode of the C_2N_2 complexed. Nevertheless, it is well known that the combination bands frequencies are poorly modelized in our calculations which prevent us from attributing this band for sure. On the other hand, if we consider that this band is shifted toward higher frequency by 3.1 cm^{-1} by comparison with C_2H_2 ν_5 mode, this shift is in good agreement with the calculated shift for the *P*-structure. However, for all other modes, the predicted shifts are too small to be observed, masked by the monomer absorption bands. Thus, we can only assume the presence of the P-complex in argon matrix.

3.4. Irradiation of C_2H_2:C_2N_2 *at* $\lambda > 120$ *nm*

Difference spectra (after-before photolysis) depict the photolysis effects found in samples C_2N_2/Ar, C_2H_2/Ar and C_2N_2/C_2H_2/Ar which are illustrated in Fig. 2 in two different areas. During the photolysis of C_2H_2:C_2N_2 in argon matrix at $\lambda > 120$ nm, we observe the decrease of the absorption bands of monomeric species (C_2H_2 and C_2N_2) and those of the complex (C_2H_2:C_2N_2). At the same time, new bands appeared (Fig. 2(b)). Most of them correspond to photolyzed monomers. Far-UV photolysis of rare gas matrix-isolated C_2N_2 (Fig. 2(c)) is known to give neutral radical $CN^{\bullet}$ [37]. In our experiment, the growth of one band located at 2046.7 cm^{-1} attributed to this radical indicates the break of the CC single bond. This break can induce the formation of at least two isomers of C_2N_2. So, the absorption bands growing at 2294.8 and 2054.2 cm^{-1} which present the same behavior during the photolysis could be attributed to the ν_1 and ν_2 vibration modes of CNCN [38]. Likewise, the absorption band observed at 1997.0 cm^{-1} during the photolysis experiment corresponds to the ν_2 vibrational mode of CNNC [37b]. However, another band is observed at 2023 cm^{-1}. Based on our previous work [24c,39], this band could come from the formation of CN^-.

Table 1. Experimental and theoretical frequency shifts in cm^{-1} ($\nu_{monomer}-\nu_{complex}$) for the acetylene, C_2N_2 and their complex (linear L and parallel P) at aug-cc-pVTZ level of theory. Calculated intensities are given in parenthesis

	Experiment			Calculation (aug-cc-pVTZ)			$\Delta\nu$ ($\nu_{monomer}-\nu_{complex}$)		
	Mode	Monomer ν, cm^{-1}	Complex ν, cm^{-1}	Monomer ν, cm^{-1}	L-complex ν, cm^{-1}	P-complex ν, cm^{-1}	Exp	*ccpVTZ*	
								L	*P*
C_2H_2	ν_1			3516.8 (0.0)	3505.1 (9.0)	3513.2 (0.1)		–11.7	–3.6
	ν_3	3289.1	3272.5	3412.1 (90.0)	3398.5 (216.7)	3408.3 (89.2)	–16.6	–13.6	–3.8
	ν_2	1973.8 (a)	1968.8	2068.5 (0.0)	2063.5 (6.1)	2066.9 (0.1)	–5.0	–5.0	–1.6
	ν_5	736.9	759.8	769.5 (98.1)	804.5 (82.2)	774.4 (111.1)	22.9	35.0	4.9
					804.5 (82.2)	773.8 (90.8)		35.0	4.3
C_2N_2	ν'_1		2345	2429.0 (0.0)	2431.9 (0.4)	2430.5 (0.1)		2.9	1.5
	ν'_3	2153.9	2160.2	2266.2 (0.01)	2270.1 (0.03)	2267.6 (0.01)	6.3	3.9	1.4
	ν'_2		860.1	883.5 (0.0)	885.0 (0.2)	883.3 (0.02)		1.5	–0.2

Notes: [a] The frequency is measured by the Raman spectroscopy

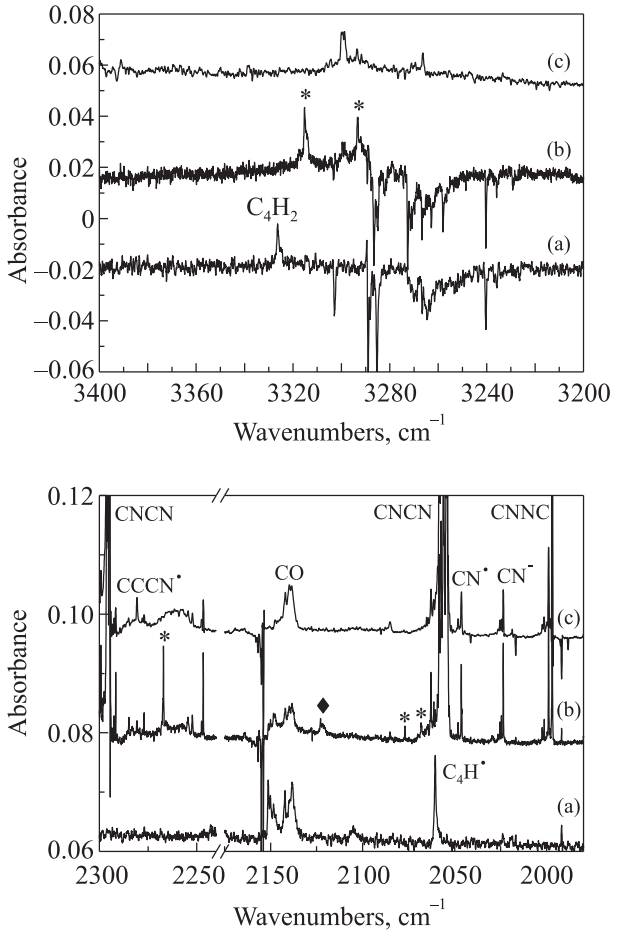

Fig. 2. FTIR difference spectra (after–before photolysis) showing the creation of photoproducts at $\lambda > 120$ nm: C_2H_2/Ar matrix, 2069 min of irradiation (a); C_2N_2/C_2H_2/Ar, 470 min (b); C_2N_2/Ar, 690 min (c). The photoproducts produced by the photochemistry of the complex are noted with an asterisk. The absorption bands coming from the photochemistry of HC_3N are noted by (♦).

By comparison with previous works, we can assign the absorption bands coming from the irradiation of acetylene. Indeed, the acetylene decomposition leads to the formation of HC_4H [40] (3326.7 cm^{-1}), $C_4H^{\bullet}$ (2060.7 cm^{-1}) [41] and $C_2H^{\bullet}$ (2846.4 cm^{-1}) [35,42]. In addition to the bands due to these species, others spectral features appeared during the irradiation, in the C–H, C≡N and C≡C triple bond stretching regions noted by an asterisk on the Fig. 2. The bands are pointed at 3314.5, 3293.3, 2268.5, 2077, 2068 and 2029 cm^{-1} and listed in Table 2. The evolution of the integrated absorbances as a function of time permits us to distinguish some sets of bands. One of these groups, composed by absorption bands at 3314.5, 2268.5 and 2077 cm^{-1} is easily identified to the cyanoacetylene on the basis of our previous work [21] as illustrated on Fig. 3. Furthermore, the band at 3293.3 cm^{-1} (Fig. 2(b)) has the same behavior, but this band cannot be attributed to HC_3N. This is seen in the Fig. 4 which depicts the intensities of 2268.5 cm^{-1} band, plotted as a function of the 3293.3 cm^{-1} band, with correlation factor of 0.99. This good correlation factor proves that the two products are formed at the same time. Likewise, based on literature data [43,44], this band appears in the ν_{CH} mode region of HCN observed in argon matrix at 3306 cm^{-1} and is shifted by 12.7 cm^{-1} towards lower frequencies with respect to the monomer. So, we can affirm that HC_3N and HCN formed during the experiment are probably trapped in the same cage. These results observed on both molecules indicate that the association of the two partners takes probably place between the nitrogen of HC_3N and the hydrogen of HCN. Vibrational theoretical calculations have been performed in order to establish the molecular structure of this complex. These calculations yield to two local minima, but the results are not in good agreement with our experiments that do not allow us to conclude which geometry of the complexes obtained in our experiment.

Table 2. Experimental frequencies in cm^{-1} of HCN, HC_3N, HC_2NC and HNC and calculated intensities given in parenthesis

HCN		HC_3N		HC_2NC		HNC	
Toumi *et al.* [24]	This work	Guennoun *et al.* [39]	This work	Guennoun *et al.* [39]	This work	Toumi *et al.* [24]	This work
3306(100)	3293.3(100)	3316(100)	3314.5(100)	3328		3620	
2098(2)		2269(18)	2268.5(36)	2213 (71)		2029	2029(100)
721(78)		2076(6)	2077(4)	2033(100)	2068(100)		

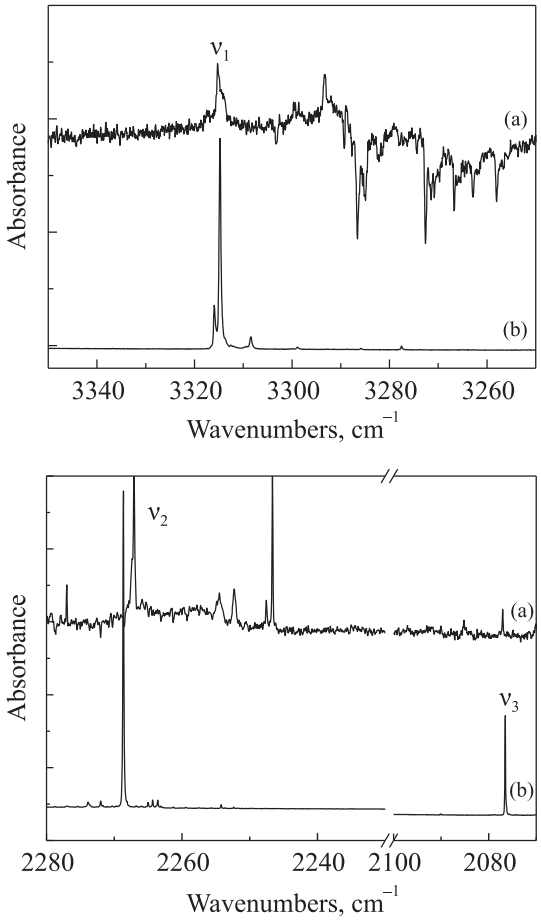

Fig. 3. FTIR difference spectra (after–before photolysis) showing the creation of photoproducts at $\lambda > 120$ nm: C_2N_2/C_2H_2/Ar, 470 min (a); HC_3N/Ar, 1/500 (b).

On the other hand, when the CC single bond of HC_3N is broken, the rotation of the $CN^{\bullet}$ group is very easy in the argon cage. This isomerization process has frequently been observed in previous experiment [45]. This kind of process leads us to suppose, the formation of HC_2NC during a secondary process. Furthermore, HC_2NC can also be formed directly during the photochemistry of the C_2H_2:C_2N_2 complex. A band is obtained at 2068 cm^{-1} during the photoprocess. This band is observed in the ν_3 range of HC_2NC [39] (2033 cm^{-1}) but is quite strongly shifted (–35 cm^{-1}) compared to the monomer. So, we can considered the possible formation of HC_2NC.

At least, one very small band is observed at 2029 cm^{-1}. Based on the literature data and on our previous works, this

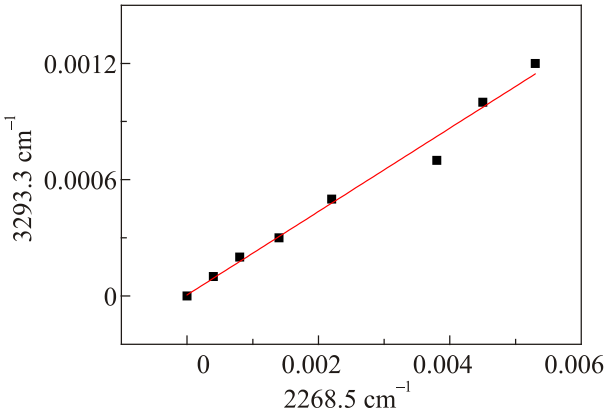

Fig. 4. Correlations between integrated optical densities IR absorption band developed during $\lambda > 120$ nm irradiation of Ar matrix-isolated C_2H_2/C_2N_2 complex at 10 K assigned to ν_2 of HC_3N (2268.5 cm^{-1}) and ν_1 of HCN (3293.3 cm^{-1}).

latter could be attributed to the formation of HNC. No other band is observed in the different areas of the spectrum. Thus, C_4N_2, its isomers, or (CN)CHCH(CN) are not formed during the photolysis process, as supposed in path 3 to 5 in Scheme 1 by addition processes.

4. Discussion

As underlined by Cherchneff *et al.* [46], it is of interest to recall that large cyanopolyynes can be produced by reaction between $C_{2n+1}N^{\bullet}$ and acetylene according to the following reaction:

$$HC_2H + C_{2n+1}N^{\bullet} \rightarrow HC_{2n+3}N + H^{\bullet}.$$

This chemistry is active in the outer envelope of the carbon rich star.

In our experimental conditions, at λ>120 nm the major process for C_2N_2 dissociation consists in the breaking of the C–CN bond leading the production of $CN^{\bullet}$ as described in Eq. (1):

$$C_2N_2 + h\nu \rightarrow 2\ {}^{\bullet}CN. \qquad (1)$$

One of this $^{\bullet}CN$ radical could then react with a nearby acetylene molecule by an addition process that results in HC_3N formation and $H^{\bullet}$ elimination in the same cage (2):

$$HC_2H + {}^{\bullet}CN + {}^{\bullet}CN \rightarrow HC_3N + H^{\bullet} + {}^{\bullet}CN. \qquad (2)$$

The transient presence of this pair of radicals ($H^{\bullet}$ and $^{\bullet}CN$) in the same cage also implies the emergence of HCN

or HNC. However, the non-detection of C_4N_2, CNC_2NC and $C_4H_2N_2$ (Scheme 1, path 3, 4 and 5) indicates that the addition of two $^{\bullet}CN$ radicals on C_2H_2 is not observed in our experimental conditions.

On the other hand, at $\lambda > 120$ nm the major process for C_2H_2 induces the production of $H^{\bullet}$ and $^{\bullet}C_2H$ after the break of the C–H bond as illustrated in (3):

$$C_2H_2 + h\nu \rightarrow {}^{\bullet}C_2H + H^{\bullet}. \quad (3)$$

Likewise, the formation of acetylenic radicals $C_2H^{\bullet}$, may be followed by an addition reaction analogous to (2) i.e :

$$H^{\bullet} + C_2H^{\bullet} + C_2N_2 \rightarrow HC_3N + CN^{\bullet} + H^{\bullet}. \quad (4)$$

So, as in the previous case, $CN^{\bullet}$ and $H^{\bullet}$ trapped in the same cage could induce the formation of HCN or HNC.

In the case of the addition of $H^{\bullet}$ on C_2N_2, the formation of HCN is expected (5)

$$C_2H^{\bullet} + H^{\bullet} + C_2N_2 \rightarrow HCN + C_2H^{\bullet} + CN^{\bullet}. \quad (5)$$

As previously mentioned, the $C_2H^{\bullet}$ and $CN^{\bullet}$ radicals trapped in the same cage can either induce the formation of HC_3N or that of HC_2NC by recombination. It is important to specify that HC_2NC can be obtain by a secondary photochemical reaction coming from the direct photochemistry of HC_3N. Indeed, it is well known that HC_3N, induces the formation of HC_2NC by isomerization process at $\lambda > 120$ nm (6):

$$HC_3N \rightarrow HC_2NC \quad (6)$$

Based on the previous discussion, the complex photochemistry provides three main channels summarized below

During the photolysis experiment at $\lambda > 120$ nm of the C_2H_2:C_2N_2 complex, the major products are the HC_3N and the HCN, which seems evident since these two molecules

$$C_2H_2 : C_2N_2 + h\nu \xrightarrow{CN^{\bullet} + C_2H_2} HC_3N + HCN \text{ or } HNC \text{ (a)}$$
$$\xrightarrow{C_2H^{\bullet} + C_2N_2} HC_3N + HCN \text{ or } HNC \text{ (b)}$$
$$\xrightarrow{H^{\bullet} + C_2N_2} HCN + HC_3N \text{ or } HC_2NC \text{ (c)}$$

can be obtained from the three processes detailed above. On the other hand, the HC_2NC formation can only come from the (c) process or by the direct photolysis of HC_3N. The observation of the very small band at 2029 cm^{-1}, corresponding at HNC can be obtained from process (a) or (b) or by direct photolysis of HCN.

However, this work suggests that HC_3N and HC_2NC could be formed during the photochemistry of C_2N_2 and C_2H_2 mixture. In previous studies, we put in evidence the formation of HC_3N from C_2H_2 and HCN [24c]. Our results seem consistent with both HC_3N training pathways as shown by different models [7] in which $CN^{\bullet}$ obtained either from HCN or C_2N_2 is predicted to react with C_2H_2 to induce the formation of HC_3N.

5. Conclusion

In this study, we have put in evidence the formation of C_2N_2–C_2H_2 complex in argon matrix by FTIR and theoretical *ab initio* calculations. The complex presents a linear structure characterized by a strong hydrogen bond between the two partners. These conclusions are supported by the good agreement between the theoretical and experimental frequency shifts of the νCH and δCCH modes of the acetylenic group. The photodissociation of C_2N_2–C_2H_2 trapped in argon matrix at 10 K has been performed at $\lambda > 120$ nm and has revealed the formation of the HC_3N:HCN complex as final reactional products and permit us to suppose the HC_2NC and HCN formation. It should be necessary to perform isotopic experiment in order to confirm the formation of this later complex. The observed processes are similar to the formerly reported *in situ* cryogenic synthesis of HC_5N from HC_3N and C_2H_2 trapped in solid argon. This method confirms one way of formation of HC_3N as predicted by the different models [7].

Acknowledgements

This work was supported by the Programme National de Planétologie (PNP). The theoretical part of this work has been conducted using the "Centre Régional de Compétence en Modélisation Moléculaire de Marseille".

1. M.S. Gudipati, R. Jacovi, I. Couturier-Tamburelli, A. Lignell, and M. Allen, *Nat. Commun.* **4**, 2 (2013).
2. a) P. Coll, D. Coscia, M.C. Gazeau, E. de Vanssay, J.C. Guillemin, and F. Raulin, *Ads. Space Res.* **16**, 93 (1995); b) E.H. Wilson and S.K. Atreya, *J. Geophys Res.* (*Planets*) **109**, E06002 (2004); c) V. Vuitton, O. Dutruit, M.A. Smith, and N. Balucani, in: *Titan: Interia, Surface, Atmosphere and Space Environment*, I. Müller-Wodarg, C.A. Griffith, and T.E. Gavens (eds.), Cambridge University Press (2012), p. 224.
3. a) S.M. Hörst, Y.H. Yoon, M.S. Ugelow, A.H. Parker, R. Li, J.A. de Gouw, and M.A. Tolbert, *Icarus* **301**, 136 (2018); b) V. Vuitton, R.V. Yelle, and M.J. McEwan, *Icarus* **191**, 722 (2007); c) J. Cui, R.V. Yelle, V. Vuitton, J.H. Waite, W.T. Kasprzak, D.A. Gell, H.B. Niemann, I.C.F. Müller-Wodarg, N. Borggren, G.G. Fletcher, E.L. Patrick, E. Raaen, and B.A. Magee, *Icarus* **200**, 581 (2009).
4. a) A. Coustenis, D.E. Jennings, and C.A. Nixon, *Icarus* **207**, 461 (2010); b) N.A. Teanby, P.G.J. Irwin, R. Kok, and C.A. Nixon, *Icarus* **202**, 620 (2009).
5. A. Coupeaud, R. Kołos, I. Couturier-Tamburelli, J.P. Aycard, and N. Pietri, *J. Phys. Chem. A* **110**, 2371 (2006).
6. N. Balucani, O. Asvany, Y. Osamura, L.C.L. Huang, Y.T. Lee, and R.I. Kaiser, *Planet. Space Sci.* **48**, 447 (2000).
7. a) M. Dobrijevic, J.C. Loison, K.M. Hickson, and G. Gronoff, *Icarus* **268**, 313 (2016); b) C.N. Keller, V.G. Anicich, and T.E. Cravens, *Planet. Space Sci.* **46**, 1157 (1998); c) V.A. Krasnopolsky, *Icarus* **236**, 83 (2014); d) P. Lavvas, *et al.*

Icarus **213**, 233 (2011); e) V. Vuitton, *et al.*, *Planet. Space Sci.* **57**, 1558 (2009).
8. S. Satyapal and R. Bersohn, *J. Phys. Chem.* **95**, 8004 (1991).
9. K.S. Shin and J.V. Michael, *J. Phys. Chem.* **95**, 5864 (1991).
10. K. Seki and H. Okabe, *J. Phys. Chem.* **97**, 5284 (1993).
11. H. Okabe, *J. Chem. Phys.* **78**, 5284 (1983).
12. H. Okabe, *J. Chem. Phys.* **75**, 2772 (1981).
13. L.J. Stief, V.J. Decarlo, and R.J. Mataloni, *J. Chem. Phys.* **42**, 3113 (1965).
14. A. Laüter, K.S. Lee, K.H. Jung, R.K. Vasta, J.P. Mittal, and H.R. Volpp, *Chem. Phys. Lett.* **358**, 314 (2002).
15. E.A.J. Wannenmacher, H. Lin, and M. Jackson, *J. Phys. Chem.* **94**, 6608 (1990).
16. S.A. Barts and B. Halpern, *Chem. Phys. Lett.* **161**, 207 (1989).
17. A.G. Maki, *J. Chem. Phys.* **43**, 3193 (1965).
18. L.H. Jones, *J. Mol. Spectr.* **45**, 55 (1973).
19. G. Herzberg, *Molecular Spectra and Molecular Structure*, Van Nostrand, New York (1966), Vol. 3.
20. S.W. North and G.E. Hall, *J. Chem. Phys.* **106**, 60 (1997).
21. I. Couturier-Tamburelli, B. Sessouma, A. Coupeaud, J.P. Aycard, and N. Piétri, *Chem. Phys.* **358**, 13 (2009).
22. N. Pietri, A. Coupeaud, J.P. Aycard, and I. Couturier-Tamburelli, *Chem. Phys.* **358**, 7 (2009).
23. Z. Guennoun, A. Coupeaud, I. Couturier-Tamburelli, N. Piétri, S. Coussan, and J.P. Aycard, *Chem. Phys.* **300**, 143 (2004).
24. a) K. Nauta and R.E. Miller, *Chem. Phys. Lett.* **346**, 129 (2001); b) P.A. Block, K.W. Jucks, L.G. Pedersen, and R.E. Miller, *Chem. Phys.* **139**, 15 (1989); c) A. Toumi, I. Couturier-Tamburelli, T. Chiavassa, and N. Pietri, *J. Phys. Chem. A* **118**, 2453 (2014).
25. N. Piétri, B. Jurca, M. Monnier, M. Hillebrand, and J.P. Aycard, *Spectrochim. Acta A* **56**, 157 (2000).
26. a) W. Hagen, G.A. Allalandolo, and J.M. Geenberg, *Astrophys. Space. Sci.* **65**, 215 (1979); b) P. Jenniskens, G.A. Baratta, A. Kouchi, M.S. De Groot, J.M. Greenberg, and G. Strazulla, *Astron. Astrophys.* **273**, 583 (1993).
27. M.J. Frisch, M.J. Trucks, H.B. Schlegel, G.E. Scuseria, M.A. Robb, J.R. Cheeseman, G. Scalmani, V. Barone, B. Menucci, G.A. Petersson, *et al.*; Gaussian 09, revision A02; Gaussian Inc.: Wallingford, CT (2009).
28. a) P. Hohenberg and W. Kohn, *W. Phys. Rev.* **136**, 864 (1964); b) W. Kohn and L. Sham, *J. Phys. Rev.* **140**, 1133 (1965).
29. a) A.D. Becke, *J. Chem. Phys.* **98**, 5648 (1993); b) C. Lee, W. Yang, and R.G. Parr, *Phys. Rev. B* **37**, 785(1988).
30. R.A. Kendall, T.H. Dunning, and R.J. Harrison, *J. Chem. Phys.* **96**, 6796 (1992).
31. a) E.S. Kline, Z.H. Kafafi, R.H. Hauge, and J.L. Margrave, *J. Am. Chem. Soc.* **107**, 7550 (1985); b) R.J. Bemish, P.A. Block, L.G. Pederson, W. Yang, and R.E. Miller, *J. Chem. Phys.* **99**, 8585 (1993); c) K. Sundararajan, K.S. Viswanathan, A.D. Kulkarni, and S.R. Gadre, *J. Mol. Struct.* **613**, 209 (2002).
32. a) C.R. Bailey and S.C. Carson, *J. Chem. Phys.* **7**, 859 (1939); b) G. Herzberg, *Molecular Spectra and Molecular Structure. Infrared and Raman Spectra of Polyatomic Molecules*, Van Nostrand, Priceton (1945), Vol II.
33. B.H. Thomas and W.J. Orville-Thomas, *J. Mol. Struct.* **3**, 191 (1969).
34. A. Langseth and C.K. Moller, *Acta Chem. Scand.* **4**, 725 (1950).
35. B. Sessouma, I. Couturier-Tamburelli, A. Allouche, and J-P. Aycard, *Chem. Phys.* **278**, 9 (2002).
36. I. Couturier-Tamburelli, B. Sessouma, A. Coupeaud, J.-P. Aycard, and N. Piétri, *Chem. Phys.* **358**, 13 (2009).
37. a) D.E. Milligan and M.E. Jacox, *J. Chem. Phys.* **47**, 278 (1967); b) M.E. Jacox, *J. Mol. Spectr.* **113**, 286 (1985).
38. a) F. Stroh and M. Winnewisser, *Chem. Phys. Lett.* **155**, 21 (1989); b) F. Stroh, B.P. Winnewisser, M. Winnewisser, H.P. Reisenauer, G. Maier, S.J. Goede, and F. Bickelhaupt, *Chem. Phys. Lett.* **160**, 2, 105 (1989).
39. Z. Guennoun, I. Couturier-Tamburelli, N. Piétri, and J.P. Aycard, *Chem. Phys. Lett.* **368**, 574 (2003).
40. a) M.E. Jacox and W.B. Olson, *J. Chem. Phys.* **86**, 3134 (1987). b) N.L. Owen, C.H. Smith, and G.A. Willliams, *J. Mol. Struct.* **161**, 33 (1987).
41. L.N. Shen, T.J. Doyle, and W.R.M. Graham, *J. Chem. Phys.* **93**, 1697 (1990).
42. W.R.M. Graham, K.I. Dismuke, and W.Jr. Weltner, *J. Chem. Phys.* **60**, 3817 (1974).
43. a) K. Satoski, M. Takayanagi, and M. Nakata, *J. Mol. Struct.* **365**, 413 (1997); b) C.M. King and E.R.J. Nixon, *Chem. Phys.* **48**, 1685 (1968).
44. Z. Guennoun, I. Couturier-Tamburelli, S. Combes, J.P. Aycard, and N. Piétri, *J. Phys. Chem. A* **109**, 11733 (2005).
45. R. Kolos and J. Waluk, *J. Mol. Struct.* **473**, 408 (1997).
46. I. Cherchneff, A.E. Glassgold, and G.A. Mamon, *Astrophys. J.* **410**, 188 (1993).

Новий можливий шлях формування HC_3N в атмосфері Титана

J. Mouzay, C. Assadourian, N. Piétri, T. Chiavassa, I. Couturier-Tamburelli

Структури комплексу C_2N_2/C_2H_2 в твердих аргонових матрицях було досліджено за допомогою FTIR спектроскопії та *ab initio* розрахунків на aug-cc-pVTZ рівні теорії. Передбачені зсуви частот для лінійної структури, яка характеризується сильним водневим зв'язком між азотом у C_2N_2 та протоном ацетилену, добре узгоджуються з експериментом. Фотодисоціація комплексу C_2N_2–C_2H_2, який локалізований в матриці аргону при 10 K, відбувалася при опроміненні світлом з довжиною хвилі 120 нм. Вимірювання FTIR та *ab initio* розрахунки вказують на утворення HC_3N, HCN і, можливо, HC_2NC та HNC кінцевих продуктів реакції. Хід реакції за цим механізмом є потенційно важливим для хімічних моделей атмосфери Титана.

Ключові слова: аргонові матриці, атмосфера Титана, FTIR спектроскопія.

Новый возможный путь формирования HC_3N в атмосфере Титана

J. Mouzay, C. Assadourian, N. Piétri, T. Chiavassa, I. Couturier-Tamburelli

Структуры комплекса C_2N_2/C_2H_2 в твердых аргоновых матрицах были исследованы с помощью FTIR спектроскопии и *ab initio* расчетов на aug-cc-pVTZ уровне теории. Предсказанные сдвиги частот для линейной структуры, характеризующейся сильной водородной связью между азотом в C_2N_2 и протоном ацетилена, находятся в хорошем согласии с экспериментом. Фотодиссоциация комплекса C_2N_2–C_2H_2, локализованного в матрице аргона при 10 K, происходила при облучении светом с длиной волны 120 нм. Измерения FTIR и *ab initio* расчет указывают на образование HC_3N, HCN и, возможно, HC_2NC и HNC конечных продуктов реакции. Ход реакции по этому механизму потенциально важен для химических моделей атмосферы Титана.

Ключевые слова: аргоновые матрицы, атмосфера Титана, FTIR спектроскопия.